Functional Role of Lipid Raft Microdomains in Cyclic Nucleotide-Gated Channel Activation

James D. Brady, Thomas C. Rich, Xuan Le, Kimberlee Stafford, Cedar J. Fowler, Leatha Lynch, Jeffrey W. Karpen, R. Lane Brown, and Jeffrey R. Martens

Department of Physiology & Pharmacology, Oregon Health & Science University, Portland, Oregon (J.D.B., X.L., K.S., C.J.F., J.W.K., J.R.M.); Department of Integrative Biology and Pharmacology, University of Texas Health Science Center at Houston, Houston, Texas (T.C.R.); and Neurological Sciences Institute, Oregon Health & Science University, Beaverton, Oregon (L.L., R.L.B.)

This article is available online at http://molpharm.aspetjournals.org

ABSTRACT

Cyclic nucleotide-gated (CNG) channels are the primary targets of light- and odorant-induced signaling in photoreceptors and olfactory sensory neurons. Compartmentalized cyclic nucleotide signaling is necessary to ensure rapid and efficient activation of these nonselective cation channels. However, relatively little is known about the subcellular localization of CNG channels or the mechanisms of their membrane partitioning. Lipid raft domains are specialized membrane microdomains rich in cholesterol and sphingolipids that have been implicated in the organization of many membrane-associated signaling pathways. Herein, we report that the α subunit of the olfactory CNG channel, CNGA2, associates with lipid rafts in heterologous expression systems and in rat olfactory epithelium. However, CNGA2 does not directly bind caveolin, and its membrane localization overlaps only slightly with that of caveolin at the surface of human embryonic kidney (HEK) 293 cells. To test for a possible functional role of lipid raft association, we treated HEK 293 cells with the cholesterol-depleting agent, methyl-β-cyclodextrin. Cholesterol depletion abolished prostaglandin E_1-stimulated CNGA2 channel activity in intact cells. Recordings from membrane patches excised from CNGA2-expressing HEK 293 cells revealed that cholesterol depletion dramatically reduced the apparent affinity of homomeric CNGA2 channels for cAMP but only slightly reduced the maximal current. Our results show that olfactory CNG channels target to lipid rafts and that disruption of lipid raft microdomains dramatically alters the function of CNGA2 channels.

Cyclic nucleotide-gated (CNG) ion channels were first discovered in retinal photoreceptors and olfactory neurons, where they modulate the membrane potential in response to stimulus-induced changes in the intracellular concentrations of cyclic nucleotides (Fesenko et al., 1985; Nakamura and Gold, 1987; Firestein and Werblin, 1989). Although CNG channels have now been found in many other neuronal and non-neuronal cells, their physiological roles in nonsensory tissues remain obscure (Finn et al., 1996). Over the past several years, however, we have learned much about the structure and functional properties of these nonselective cation channels (Kaupp and Seifert, 2002). To date, six CNG channel subunits have been cloned, including both α (CNGA1–4) and β (CNGB1 and 3) subunits. Although many of the α-subunits can be functionally expressed as homomul- timers, coexpression of the β-subunits is known to confer distinct functional properties, in terms of ion permeation, ligand sensitivity, gating mechanisms, and regulation. Recent evidence suggests that the stoichiometry of the native rod photoreceptor channel is three CNGA1 to one CNGB1 (Weitz et al., 2002; Zheng et al., 2002; Zhong et al., 2002). The native olfactory channel is thought to contain three subunit types, including CNGA2, CNGA4, and CNGB1.3, although the stoichiometry remains unknown (Bradley et al., 1994; Liman and Buck, 1994; Sautter et al., 1998; Bonigk et al., 1999).

Despite a relative wealth of knowledge about CNG channel structure and function, very little is known about the mechanisms responsible for their targeting and subcellular localization. Because a growing number of channel-linked genetic diseases involve the failure of channels to reach the cell surface (Griffith, 2001), the general mechanisms of ion channel targeting are of considerable interest. The importance of

ABBREVIATIONS: CNG, cyclic nucleotide-gated; OSN, olfactory sensory neurons; GFP, green fluorescent protein; CFP, cyan fluorescent protein; CD, methyl-β-cyclodextrin; CPT, 8-(p-chlorophenylthio); HEK, human embryonic kidney; MES, 2-(N-morpholino)ethanesulfonic acid; PBS, phosphate-buffered saline; PAGE, polyacrylamide gel electrophoresis; DRM, detergent-resistant membrane; PG, prostaglandin.

CNG channel targeting is illustrated by a recent report showing that the trafficking of rod CNG channels to the plasma membrane is disrupted in an inherited form of blindness (Trudeau and Zagotta, 2002). In photoreceptors and OSNs, the targeting of CNG channels to very specific regions of the plasma membrane rich in sensory signaling molecules allows for efficient and spatially confined responses to sensory stimuli (Baylor et al., 1979; Nakamura and Gold, 1987; Firestein and Werblin, 1989; Savchenko et al., 1997).

It has been shown that several proteins involved in sensory signaling in photoreceptors and OSNs reside in specialized plasma membrane subdomains called lipid rafts (Seno et al., 2001; Schreiber et al., 2000). These physically distinct membrane regions are rich in particular lipids, especially sphingolipids and cholesterol, and they concentrate certain membrane proteins, including signal transduction enzymes, membrane receptors, and ion channels (Simons and Ikonen, 1997; Brown and London, 1998; Martens et al., 2000). Lipid rafts are thought to facilitate the lateral assembly of signaling cascades (Simons and Toomre, 2000), whereas depletion of raft lipids is known to disrupt a number of signaling events, such as T-cell activation (Magee et al., 2002) and β-adrenergic signaling (Rybin et al., 2000).

Here we report for the first time that the primary subunit of the olfactory CNG channel, CNGA2, is localized to lipid rafts in both heterologous expression systems and in native olfactory tissue. Depleting membrane cholesterol to perturb lipid rafts dramatically altered the function of homomeric CNGA2 channels in intact cells and isolated patches. Our results show that the integrity of the cholesterol-rich lipid environment is an important modulator of raft-localized CNGA2 channel function. Furthermore, these results support the idea that local membrane environment is important for maintaining protein-lipid interactions necessary for transmembrane signaling.

Materials and Methods

Materials. A mouse monoclonal antibody (CRO2H7) was raised against the C-terminal region of rat CNGA2 (amino acids Y482–E664) fused to a maltose binding protein. Immunization of C57BL/6 mice and fusion of immune spleen cells were performed according to standard procedures. Anti-FLAG M2 monoclonal antibody was obtained from Sigma. Polyclonal antibodies raised against caveolin that recognize all 3 caveolin isoforms were from BD Transduction Laboratories (Lexington, KY); monoclonal antibodies against the human transferrin receptor were from Zymed (South San Francisco, CA); and polyclonal antibodies against GFP were from BD Biosciences Clontech (Palo Alto, CA). Prostaglandin E$_1$ (PGE$_1$) was obtained from Calbiochem (San Diego, CA); forskolin, methyl-β-cyclodextrin (CD), and 8-(p-chlorophenylthio)-cGMP (CPT-cGMP) were from Sigma-Aldrich (St. Louis, MO). An adenovirus construct encoding a CNGA2 channel with the mutations C460W and E583M was described previously (Rich et al., 2001b). The wild-type CNGA2 in a pCIS vector was a gift from R. Reed (Johns Hopkins University, Baltimore, MD). The 3XFLAG-CNGA2 was made by inserting the wtCNGA2 into the p3xFLAG-CMV-7.1 vector (Sigma). CFP-CNGA2 was made by inserting the wtCNGA2 gene into the p-ECFPC1 vector (BD Biosciences Clontech).

Cell Culture, Transfection, and Infection. Human embryonic kidney (HEK) 293 and COS-1 cells were maintained in 100-mm culture dishes in Dulbecco's modified Eagle's medium supplemented with 10% fetal bovine serum, 2% penicillin/streptomycin (Invitrogen, Carlsbad, CA) and 0.1% Gentamicin (Invitrogen) at 37°C in a hu-

midified atmosphere of 95% air/5% CO$_2$. Cells were transfected at 60 to 80% confluence with 3 μg of DNA combined with 25 μl of LipofectAMINE reagent (Invitrogen) in serum-free Dulbecco's modified Eagle's medium for 6 to 7 h and used for experiments 18 to 48 h after return to serum-supplemented media.

Adenoviral infection of HEK 293 cells was performed as described previously (Rich et al., 2000; Rich et al., 2001a,b). Cells were detached from dishes with phosphate-buffered saline containing 0.03% EDTA 24 h after infection, resuspended in serum-supplemented media, and assayed for CNGA2 channel activity within 12 h.

Detergent Extraction and Cholesterol Depletion. To assess detergent insolubility, cells from a single confluent 100 mm culture dish were homogenized in MES-buffered saline (25 mM MES, pH 6.5, 150 mM NaCl) containing 1% Triton X-100. The homogenate was then centrifuged at 13,400 rpm in a microcentrifuge at 4°C for 30 min. After removal of the supernatant, the pellet was resuspended in phosphate-buffered saline (PBS), and both the pellet and supernatant were mixed with SDS-PAGE sample buffer.

Isolation of low-density, Triton X-100–insoluble complexes was performed essentially as described previously (Martens et al., 2000). Briefly, confluent cells from a single 100-mm dish were homogenized in MES-buffered saline containing 1% Triton X-100 (unless otherwise indicated), and sucrose was added to a final concentration of 40%. A 5-to-30% discontinuous sucrose gradient was layered on top of this detergent extract followed by ultracentrifugation [54,000 rpm in a rotor (Beckman Coulter, Fullerton, CA)] for 18 to 24 h at 4°C in a TL-100 ultracentrifuge (Beckman Coulter). Successive gradient fractions were collected from the top and subjected to SDS-PAGE and Western blot analysis. Cholesterol depletion was achieved by incubating cells for 1 h in 2% methyl-β-cyclodextrin in serum-free media at 37°C, with shaking every 5 min.

Preparation of crude olfactory membranes was performed by scraping the epithelial lining from the nasal turbinates into a sucrose phosphate solution containing protease inhibitors and centrifuged at 1000 rpm to remove bone or cartilage. The pellet was removed and the supernatant was centrifuged at 13,000 rpm in a Beckman Coulter JA25.5 rotor. The resulting pellet was resuspended in PBS. Raft preparations of rat nasal membranes were performed with 3% Triton X-100. For deglycosylation, samples of rat nasal membranes containing 20 μg of protein were incubated with 500 units of N-glycosidase F (New England Biolabs, Beverly, MA) for 1 h at 37°C.

Protein and Cholesterol Measurements. The protein concentration of sucrose gradient fractions was determined with a Bradford protein assay kit (Bio-Rad, Hercules, CA). The total cholesterol in density-gradient fractions was determined using a liquid chromatography-mass spectroscopy (MS) protocol developed by the Pharmacokinetics Core Laboratory in the Department of Physiology and Pharmacology at Oregon Health and Science University. After addition of 1000 ng of d$_6$-cholesterol as an internal standard, fractions were hydrolyzed with ethanolic potassium hydroxide at 100°C for 5 min and cholesterol was then extracted in hexane. Positive atmospheric pressure chemical ionization-MS with an ion trap mass spectrometer (LCQ Advantage; Thermo Finnigan, San Jose, CA) gave a predominant ion for cholesterol at 369 [MH$^+$-H$_2$O]. A tandem MS transition from 369 to 243 was monitored in a selected-reaction monitoring scan event (for d$_6$-cholesterol, the transition from 375 to 249 was monitored). The atmospheric pressure-chemical ionization interface was operated using the following settings: sheath and aux gas flow rates, 70 and 29, respectively; vaporizer temperature, 450°C; and capillary temperature, 225°C. Cholesterol concentrations were calculated by comparing the area ratio of unknowns to standard curves generated with cholesterol oleate (0–2000 ng) and 1000 ng of d$_6$-cholesterol.

Immunoprecipitation. HEK 293 cell membranes or rat nasal membranes were solubilized in 10 mM Tris, pH 8.0, 150 mM NaCl, 1% Triton X-100, and 60 mM octyl-glucoside, supplemented with protease inhibitors (complete tablets; Roche). After incubation for 45

min at 4°C, the solubilized membranes were centrifuged in a microcentrifuge at 13,400 rpm for 15 min at 4°C. Solubilized membranes were incubated with polyclonal anti-caveolin (1:500) or monoclonal anti-CNGA2 (1:250) antibody overnight at 4°C with gentle mixing. The next day, 250 μl of a 1:5 dilution of Sepharose-conjugated protein A (anti-caveolin) or protein G (anti-CNGA2) beads (Sigma) was added, and the samples were incubated for 3 h at 4°C with gentle mixing. The beads with bound antibody-antigen complex were pelleted and washed three times with 0.5% Triton X-100, 150 mM NaCl, 50 mM Tris-Cl, pH 7.5, 1 mM EDTA, followed by a wash in 1% Triton X-100. The final pellet was resuspended in 40 μl of PBS and SDS-PAGE sample buffer, briefly centrifuged to remove the beads, then subjected to SDS-PAGE and Western Blot anaylsis.

Immunostaining. Immunofluorescent labeling of caveolin was performed essentially as described previously (Martens et al., 2000). Cells were fixed and permeabilized before incubation with anti-caveolin antibodies (1:500). After incubation in biotinylated secondary antibody (1:200), the staining was visualized with a Cy3-conjugated streptavidin (1:500). The secondary antibody and streptavidin were obtained from Jackson Immunoresearch Laboratories Inc. (West Grove, PA). Imaging was performed on a Zeiss Axiovert 200 M microscope equipped with standard epifluorescence and a Photometrics Cool Snap HQ charge-coupled device camera (Roper Scientific, Trenton, NJ).

Detection of CNG Channel Activity in Cell Populations. The fluorescent indicator fura-2 was used to monitor Ca^{2+} influx through CNGA2 channels in cell suspensions. HEK 293 cells were infected with an adenovirus construct encoding a CNGA2 channel containing two mutations, C460W and E583M, that increase cAMP sensitivity and decrease cGMP sensitivity, respectively (Rich et al., 2001a,b). The loading of cells with fura-2 and the assay of calcium influx has been described in detail (Rich et al., 2001b). After fura-2 loading, some cells were exposed to 2% CD for 1 h or 2% CD along with 1 mM cholesterol as described previously (Furuchi and Anderson, 1998), whereas control cells were otherwise treated identically.

Patch Clamp Recordings. Electrodes had tip resistances between 1.5 and 3 MΩ when filled with a solution containing 140 mM NaCl, 5 mM KCl, 0.5 mM EDTA, and 10 mM HEPES, pH 7.4. HEK 293 cells were transfected with plasmids encoding wtCNGA2 and soluble enhanced GFP using Effectene (QIAGEN, Valencia, CA), and plated on glass coverslips coated with poly-L-lysine. After an average of 2 days, inside-out patches were pulled from GFP-positive cells either before or after treatment with 2% CD for 15 to 30 min at 37°C in extracellular bath solution containing 140 mM NaCl, 5 mM KCl, 5 mM MgCl$_2$, 2 mM CaCl$_2$, and 10 mM HEPES, pH 7.4. Currents were activated by bath application of increasing concentrations of cAMP (5 to 5000 μM) in a solution containing 140 mM KCl, 5 mM NaCl, 0.5 mM EDTA, and 10 mM HEPES, pH 7.4, and dose-response curves were measured at + 50 mV as described previously (Rich et al., 2000). All currents were normalized to a maximal patch current recorded in 1 mM cGMP.

Results

CNGA2 Associates with Lipid Rafts in Heterologous Expression Systems and Olfactory Tissue. Lipid rafts are experimentally characterized by their resistance to solubilization by nonionic detergents, such as Triton X-100, and a low buoyant density (Brown and London, 1998). We first examined the detergent insolubility of CNGA2 in a heterologous expression system. HEK 293 cells were transiently transfected with a CNGA2 construct tagged at the N terminus with the 3XFLAG epitope. When transfected cells were extracted at 4°C with buffer containing 1% Triton X-100, FLAG-CNGA2 was found primarily in the detergent-insoluble pellet (Fig. 1A). Detergent insolubility can arise from associations with detergent-resistant membranes, such as

lipid rafts, or through interactions with large protein complexes, such as the cytoskeleton. To investigate the possibility of a cytoskeletal interaction, we treated cell homogenates with high salt (0.6 M potassium iodide) to disrupt protein-protein interactions. Treatment of the Triton X-100 cell extracts with potassium iodide did not solubilize CNGA2 (Fig. 1A), suggesting that CNGA2 was associated with detergent-resistant membranes.

To determine whether CNGA2 partitions into lipid raft microdomains, we examined the density of the insoluble membrane fragments containing CNGA2. HEK 293 cells expressing FLAG-CNGA2 were extracted with 1% Triton X-100 at 4°C, and the resulting extracts were layered on the bottom of a discontinuous sucrose gradient and subjected to equilibrium density centrifugation. Immunoblotting of gradient fractions revealed two peaks of CNGA2 immunoreactivity (Fig. 1B). A significant percentage of FLAG-CNGA2 was found in buoyant detergent-insoluble fractions at the interface between the 5 and 30% sucrose layers. Under these
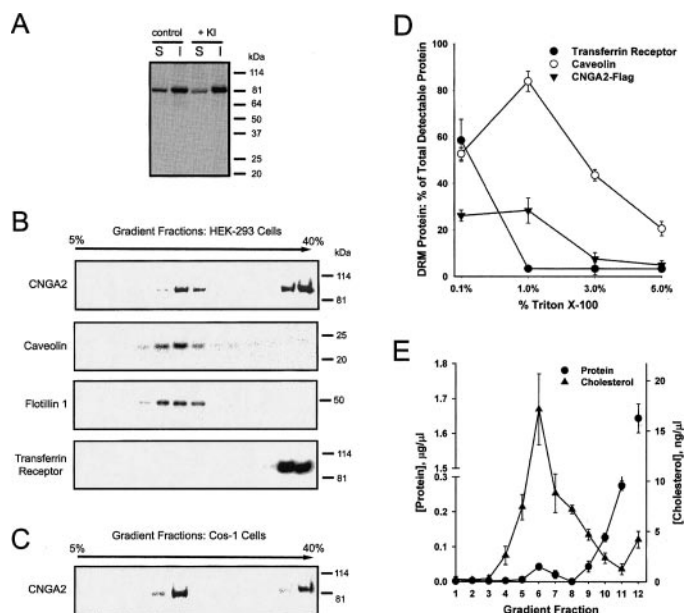

Fig. 1. CNGA2 localizes to lipid rafts in heterologous expression systems. A, cell lysates from HEK 293 cells transiently transfected with FLAG-CNGA2 were homogenized in 1% Triton X-100 with or without 0.6 M KI to disrupt protein-protein interactions. Western blots of detergent-soluble (S) and -insoluble (I) proteins were probed with anti-FLAG antibody. FLAG-CNGA2 appears as a sharp band at approximately 85 kDa. The presence of 0.6 M KI during homogenization had no effect on the solubility of CNGA2 in Triton X-100. B and C, sucrose density gradient centrifugation of 1% Triton X-100 solubilized extracts from HEK 293 cells (B) or COS-1 cells (C) expressing FLAG-CNGA2 were prepared as described under *Materials and Methods*. Western blots probed with anti-FLAG demonstrate that CNGA2 is present in detergent-insoluble, low-density lipid raft fractions, which are also enriched in endogenous caveolin and flotillin 1 but lack endogenous transferrin receptor. Shown is a representative example from four experiments. 5% and 40% refer to the sucrose concentration at the top and bottom of the gradient, respectively. D, DRM were isolated by homogenizing HEK 293 cells in different concentrations of Triton X-100 and subjecting the lysates to sucrose density gradient centrifugation. Western blots of gradient fractions were probed with appropriate antibodies. The integrated optical density of detectable protein in the low-density fractions was measured using Labworks software (UVP, Inc., Upland, CA), then expressed as a percentage of the total detectable protein along the entire gradient (error bars represent S.E.M., $n = 3$). E, after homogenization of HEK 293 cells in 1% Triton X-100 and sucrose density gradient centrifugation, the protein and cholesterol content of each gradient fraction was determined as described under *Materials and Methods* (error bars represent S.E.M., $n = 3$).

conditions, the CNGA2 subunit comigrated with the raft marker proteins caveolin (Anderson, 1998), flotillin 1, and flotillin 2 (data not shown) in the low-density fractions (Fig. 1B). FLAG-CNGA2 protein was also present in the high-density, detergent-soluble fractions at the bottom of the gradient, which is most probably caused by the intracellular accumulation of overexpressed protein (Martens et al., 2000). Similar results were obtained with COS-1 cells (Fig. 1C), indicating that raft association was independent of the cell type chosen for heterologous expression. Homogenizing cells with 60 mM octylglucoside, which effectively solubilizes detergent-resistant raft membranes (Shogomori and Brown, 2003), resulted in the nearly complete solubilization of CNGA2 as evidenced by the loss of immunoreactivity in the low-density fractions (data not shown).

When assessing raft affinity using detergents, it is critical to choose a detergent concentration that effectively separates detergent-insoluble membranes from detergent-soluble membranes and proteins. To ensure against incomplete solubilization of nonraft proteins, the transferrin receptor, which is not associated with lipid rafts (Smart et al., 1995; Harder et al., 1998; Shogomori and Brown, 2003), was used as a marker for Triton X-100 soluble membranes in each experiment (Fig. 1B). The effects of Triton X-100 concentration on detergent-resistant membrane (DRM) recovery in our system was determined by comparing extraction at several different concentrations of detergent (Fig. 1D). With 1% Triton X-100 in the homogenization buffer, approximately 80% of cellular caveolin and 25% of CNGA2 channel protein was detected in raft fractions whereas endogenous transferrin receptor was completely solubilized. Importantly, lowering the Trition X-100 concentration to 0.1% resulted in under-solubilization of cellular membranes, and approximately 50% of the transferrin receptor was now detected in the low-density fractions along with caveolin and CNGA2. Increasing the detergent concentration to 3 or 5% significantly solubilized caveolin. These results demonstrate that 1% Triton X-100 effectively separated DRMs from detergent soluble membranes in our preparation. In addition, at this detergent concentration a very small amount of total cellular protein (approximately 4%) was recovered in the DRMs, whereas these fractions contained the majority (approximately 70%) of cellular cholesterol (Fig. 1E). Although it is important to note that this assay is only a qualitative measure of a protein's DRM affinity and not a quantitative measure of raft association (Shogomori and Brown, 2003), together these experiments show that heterologously expressed CNGA2 associates with cholesterol-rich, detergent resistant membranes.

In OSNs, CNG channels containing the CNGA2 subunit are concentrated in the dendritic cilia where they generate an electrical signal in response to odorant-stimulated production of cAMP (Nakamura and Gold, 1987). To determine whether endogenous CNGA2 was associated with lipid rafts, we used an antibody against the wild-type subunit (kind gift of Dr. U. Benjamin Kaupp). To confirm specificity, we probed Western blots containing membranes from untransfected HEK 293 cells or cells transiently expressing wtCNGA2, FLAG-CNGA2 or CFP-CNGA2. The results indicate that the anti-wtCNGA2 antibody recognizes both the wild-type and epitope-tagged forms of the CNGA2 subunit with very little background staining (Fig. 2A). In OSNs, CNGA2 exists predominantly in a highly glycosylated form, and the carbohy-

drate moiety can be removed by enzymatic digestion (Bonigk et al., 1999), as illustrated in Fig. 2B. Western blot analysis of sucrose gradient fractions from detergent-extracted rat nasal membranes revealed that the glycosylated form of CNGA2 was present in buoyant lipid raft fractions (Fig. 2C). Again, these buoyant fractions were rich in caveolin but contained no transferrin receptor. These results indicate that a portion of native olfactory CNG channels associates with lipid rafts in olfactory membranes. The sizeable percentage of CNG channel found at the bottom of the gradient might reflect the existence of multiple channel populations (see Fig. 5C) or the expression of CNG channels in different cell types. Again, it should be noted, however, that the biochemical isolation of DRMs is useful as a qualitative, not a quantitative, measure of protein affinity for raft domains (Ostermeyer et al., 1999; Shogomori and Brown, 2003). Importantly, these results indicate that CNGA2/raft association is not an arti-
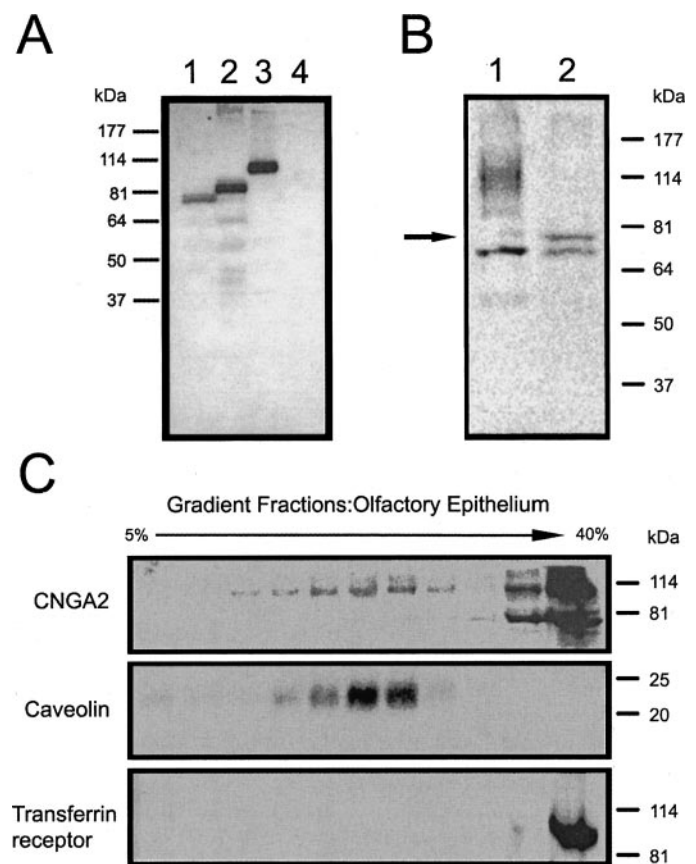

Fig. 2. Glycosylated CNGA2 localizes to lipid rafts in membranes from rat olfactory tissue. A, cellular membranes prepared from HEK 293 cells transiently transfected with wtCNGA2 (lane 1), FLAG-CNGA2 (lane 2), or CFP-CNGA2 (lane 3), and membranes from untransfected HEK 293 cells (lane 4) were subjected to SDS-PAGE, transferred to nitrocellulose, and probed with an antibody raised against native CNGA2. B, membranes prepared from rat nasal tissue were subjected to SDS-PAGE before (lane 1) or after (lane 2) incubation with N-glycosidase F for 1 h at 37°C. Western blot analysis demonstrates that the anti-CNGA2 antibody recognizes glycosylated CNGA2 (smear centered at 114 kDa in lane 1) as well as the nonglycosylated form of CNGA2 at approximately 75 kDa, indicated by the arrow (lane 2). The lowest band in both lanes is a nonspecific band stained by the secondary antibody alone. C, Western blot of sucrose density gradient fractions of 3% Triton X-100 extracted rat olfactory membranes probed for CNGA2, caveolin, and transferrin receptors. Glycosylated CNGA2 is clearly present in low-density lipid raft fractions ($n = 3$). 5% and 40% refer to the sucrose concentration at the top and bottom of the gradient, respectively.

fact of heterologous expression. Although only the glycosylated form of CNGA2 was detected in the detergent-resistant gradient fractions, our data in heterologous expression systems suggest that glycosylation is not necessary for the association of CNGA2 with raft domains. This idea is consistent with previous work demonstrating that glycosylation is not a signal for raft association (Benting et al., 1999; Bravo-Zehnder et al., 2000).

CNGA2 Associates with Predominantly Noncaveolar Lipid Rafts in Heterologous Expression Systems. Previous work implicates caveolin in the regulation of odorant signaling (Schreiber et al., 2000), and caveolar and noncaveolar raft domains are known to play different roles in the regulation of membrane signaling (Sowa et al., 2001). The biochemical isolation of lipid rafts does not, however, distinguish between caveolar and noncaveolar lipid raft membranes. Therefore, we performed additional experiments to determine whether CNGA2 associates with caveolae in native membranes and heterologous expression systems.

Although CNGA2 cofractionates with caveolin in detergent-resistant sucrose gradient fractions, immunoprecipitation experiments gave no evidence that CNGA2 and caveolin directly interact in either HEK 293 cells (Fig. 3A) or in olfactory membranes (Fig. 3B). In addition, fluorescence microscopy revealed incomplete colocalization of the two proteins at the cell surface (Fig. 3, C-E). Similar results were obtained for flotillin 1 and 2 (data not shown). Based on these results, we conclude that CNGA2 is found predominantly in noncaveolar lipid raft domains at the plasma membrane.

Cholesterol Depletion Disrupts the Association of CNGA2 with Lipid Rafts and Alters Channel Function. Given that lipid rafts are enriched in cholesterol and sphingolipids, their integrity is sensitive to exogenously applied lipid-depleting agents (Brown and London, 1998). Before detergent extraction, we treated HEK 293 cells expressing FLAG-CNGA2 for 1 h with the membrane-impermeant cholesterol-binding agent CD. This treatment is commonly used to disrupt lipid raft integrity (Simons and Toomre, 2000). Gas chromatography and mass spectrometry analysis demonstrated that 2% CD pretreatment of HEK 293 cells for 1 h produced a 90% decrease in total cellular cholesterol (data not shown). Western blot analysis of sucrose gradient fractions from CD-pretreated cells demonstrated that cholesterol depletion reduced the buoyancy of CNGA2 lipid raft membranes (Fig. 4). The peak of buoyant CNGA2 immunoreactivity was shifted down the gradient, and increased levels of CNGA2 were found in higher density fractions. This pattern was characteristic of all cyclodextrin experiments ($n = 3$). A similar gradient pattern was observed for caveolin, consistent with previous reports (Sowa et al., 2001; Foster et al., 2003). These results indicate that CD pretreatment significantly depletes cellular cholesterol and perturbs the integrity of CNGA2-rich lipid raft membranes.

We next examined the functional significance of raft association by measuring prostaglandin E_1 (PGE_1) -stimulated CNGA2 channel activity before and after cholesterol depletion. The fluorescent indicator fura-2 was used to monitor channel-mediated Ca^{2+} influx in HEK 293 cell populations expressing a modified CNGA2 channel with increased sensitivity to cAMP (Rich et al., 2001a,b). Stimulation of cells with PGE_1 (100 nM) resulted in a rapid rise in intracellular calcium followed by a slower decline to a steady state (Fig. 5A).

Several lines of evidence indicate that this response is caused by a rise and fall in cAMP near the membrane (Rich et al., 2001a). For example, cells not expressing CNGA2 showed no significant PGE_1-stimulated increase in intracellular calcium. Surprisingly, pretreatment of cells with 2% CD nearly abolished the PGE_1-stimulated increase in CNGA2 channel activity (Fig. 5, A and E) without affecting basal calcium levels. These results are summarized in Fig. 5E, in which the rate of calcium influx was calculated as the slope of the rising phase and plotted for each condition. When cells were pretreated with both 2% CD and 1 mM cholesterol, no loss of PGE_1-stimulated calcium influx was observed (Fig. 5B). This suggests that the loss of PGE_1-stimulated channel activity
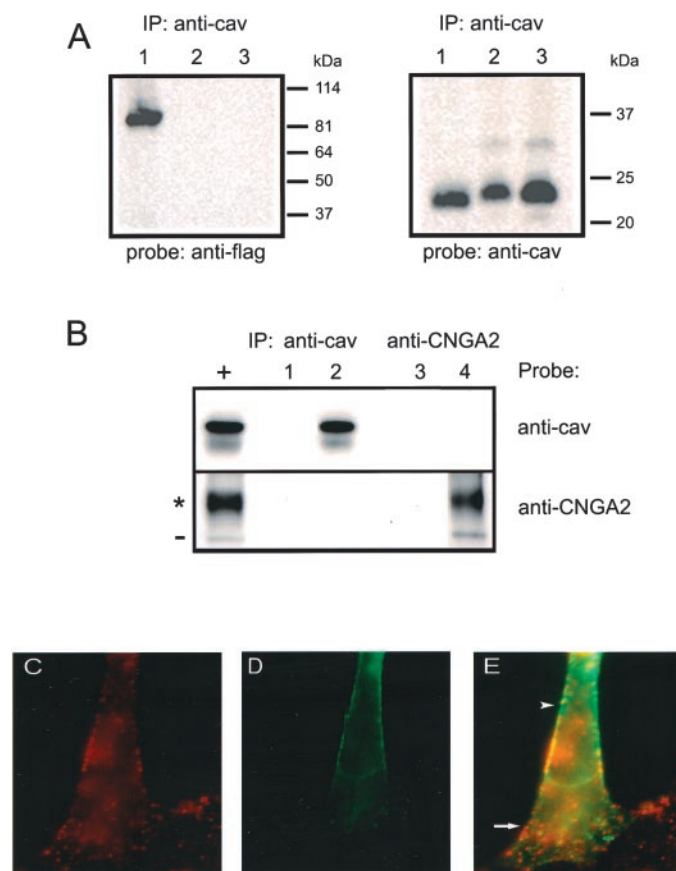

Fig. 3. CNGA2 does not directly bind caveolin and is only partially colocalized with caveolin at the surface of HEK 293 cells. A, solubilized membranes from HEK 293 cells transfected with FLAG-CNGA2 (lane 2) and from untransfected HEK 293 cells (lane 3) were immunoprecipitated with anti-caveolin antibodies. Western blots of immunoprecipitates were probed with anti-FLAG and anti-caveolin antibodies. Lane 1 contains membranes from transfected cells as a positive protein control. The results demonstrate that caveolin (~23 kDa) does not immunoprecipitate CNGA2 (85 kDa). B, solubilized membranes from rat nasal tissue (200 μg) were immunoprecipitated with anti-caveolin (lane 2), anti-CNGA2 (lane 4), or no primary antibodies (lanes 1 and 3). Western blots of the immunoprecipitates were probed with both anti-caveolin and anti-CNGA2 antibodies. Both the glycosylated (*) and unprocessed (−) forms of CNGA2 were precipitated with the anti-CNGA2, but not the anti-caveolin antibody. Rat nasal membranes (20 μg) were loaded to determine the level of caveolin and CNGA2 immunoreactivity before immunoprecipitation (+). The IP efficiency was approximately 20%. C–E, HEK 293 cells transiently expressing CFP-CNGA2 were immunofluorescently labeled with anti-caveolin antibody (1:500) and a Cy3-conjugated fluorochrome. Individual images were pseudocolored red for caveolin (C) and green for CNGA2 (D). The overlap (yellow in E) between caveolin and CNGA2 at the cell surface is limited.

after CD pretreatment is caused specifically by the depletion of cholesterol.

The dramatic loss of PGE_1-stimulated CNGA2 channel activity after cholesterol depletion could reflect a decrease in cAMP accumulation. Therefore, we measured whole-cell cAMP levels after cholesterol depletion using an enzyme immunoassay (Amersham Biosciences, Piscataway, NJ). Although 5 μM forskolin produced a measurable rise in whole-cell cAMP, 100 nM PGE_1 produced no detectable increase in whole-cell cAMP (data not shown). The finding that 100 nM PGE_1 generated a robust increase in Ca^{2+} influx without altering whole-cell cAMP levels reflects the fact that cAMP accumulates to higher concentrations in diffusionally-restricted microdomains near the surface membrane, and that CNG channels monitor cAMP levels in this pool (Rich et al., 2000, 2001a). Thus, conventional cAMP assays do not have the sensitivity to determine whether cAMP accumulation was significantly affected.

On the other hand, a decrease in channel expression or function may contribute to the dramatic loss of PGE_1-stimulated CNGA2 channel activity after cholesterol depletion. Treatment of CNGA2-expressing cells with a membrane permeant form of cGMP (CPT-cGMP) produced a sustained increase in calcium influx that was not significantly reduced by a 1-h pretreatment with 2% CD (Fig. 5, C and E). Similar treatment of uninfected cells produced no significant rise in intracellular calcium levels (Fig. 5D). These data indicate that the expression of CNGA2 channels at the cell surface and the maximal conductance were largely unaffected by cholesterol depletion. Because the maximal current is a product of the number of channels, the single-channel open probability, and the maximal single channel current ($I = Np_oi$), we set out to determine whether CD altered CNGA2 channel activity evoked by subsaturating cAMP concentrations. We therefore measured the dose-response relations of homomeric CNGA2 channels for cAMP in inside-out patches pulled from HEK 293 cells expressing wtCNGA2. Without CD pretreatment, CNGA2 channels exhibited an average

$K_{1/2}$ for cAMP of 39 μM, and a saturating concentration of cAMP elicited the same maximal current as a saturating concentration of cGMP (1 mM). Pretreatment with 2% CD profoundly decreased the apparent affinity for cAMP ($K_{1/2}$ = 123 μM) but only slightly reduced the maximal current in saturating cAMP by approximately 20% (compare saturating cGMP, Fig. 6). If the $K_{1/2}$ values for individual patches are calculated and then averaged such that each patch is weighted equally, the difference is even greater (control, $K_{1/2}$ = 42 ± 6 μM; cyclodextrin, $K_{1/2}$ = 173 ± 36 μM). Interestingly, there was high variability in this effect across patches; some patches showed very little effect and others showed a large shift in the dose-response relation. Although this variability may be a result of nonuniform cholesterol extraction between cells, it may also reflect the existence of multiple channel populations. The extremes of this variation are represented in the inset of Fig. 6.

Discussion

The results presented in this manuscript demonstrate for the first time that an α subunit of the olfactory CNG channel, CNGA2, associates with lipid rafts in both heterologous expression systems and membranes from rat nasal tissue. This association does not seem to involve caveolin but does rely on the presence of membrane cholesterol. In biochemical preparations, cholesterol depletion reduced the buoyancy of membrane fractions containing CNGA2. Depletion of plasma membrane cholesterol also dramatically reduced PGE_1-stimulated channel activity in intact cells, in part by causing a 3-fold decrease in the apparent affinity of CNGA2 channels for cAMP. At low, physiologically relevant cAMP concentrations, the 3-fold shift in the average apparent affinity could result in roughly a 9-fold change in CNG channel activity because of the cooperative nature of channel gating. This effect might be even greater given that these numbers reflect the average change, and some experiments showed a much
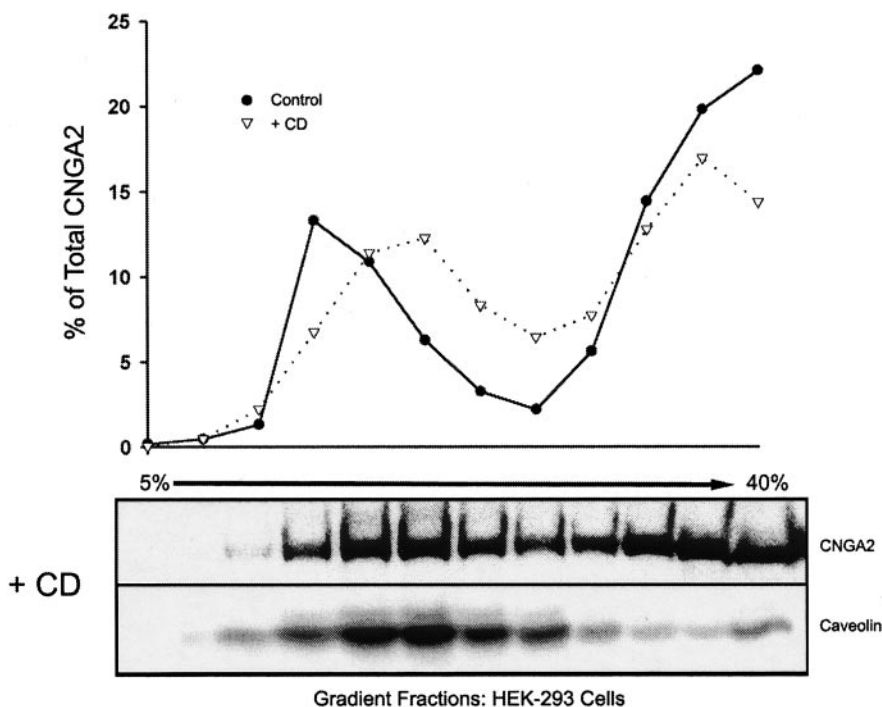

Fig. 4. Cholesterol depletion increases the density of CNGA2-containing lipid raft membranes. HEK 293 cells expressing FLAG-CNGA2 were treated with 2% CD before solubilization in 1% Triton X-100 and sucrose density centrifugation. Western blots of sucrose gradient fractions were probed with anti-FLAG and anti-caveolin antibodies, and the optical density of CNGA2 immunoreactivity in each lane was measured and expressed as a percentage of the total CNGA2 optical density. 5% and 40% refer to the sucrose concentration at the top and bottom of the gradient, respectively. Compared with results from untreated controls (●, see Fig. 1), CD produced a smear of CNGA2 immunoreactivity (▽) through the gradient.
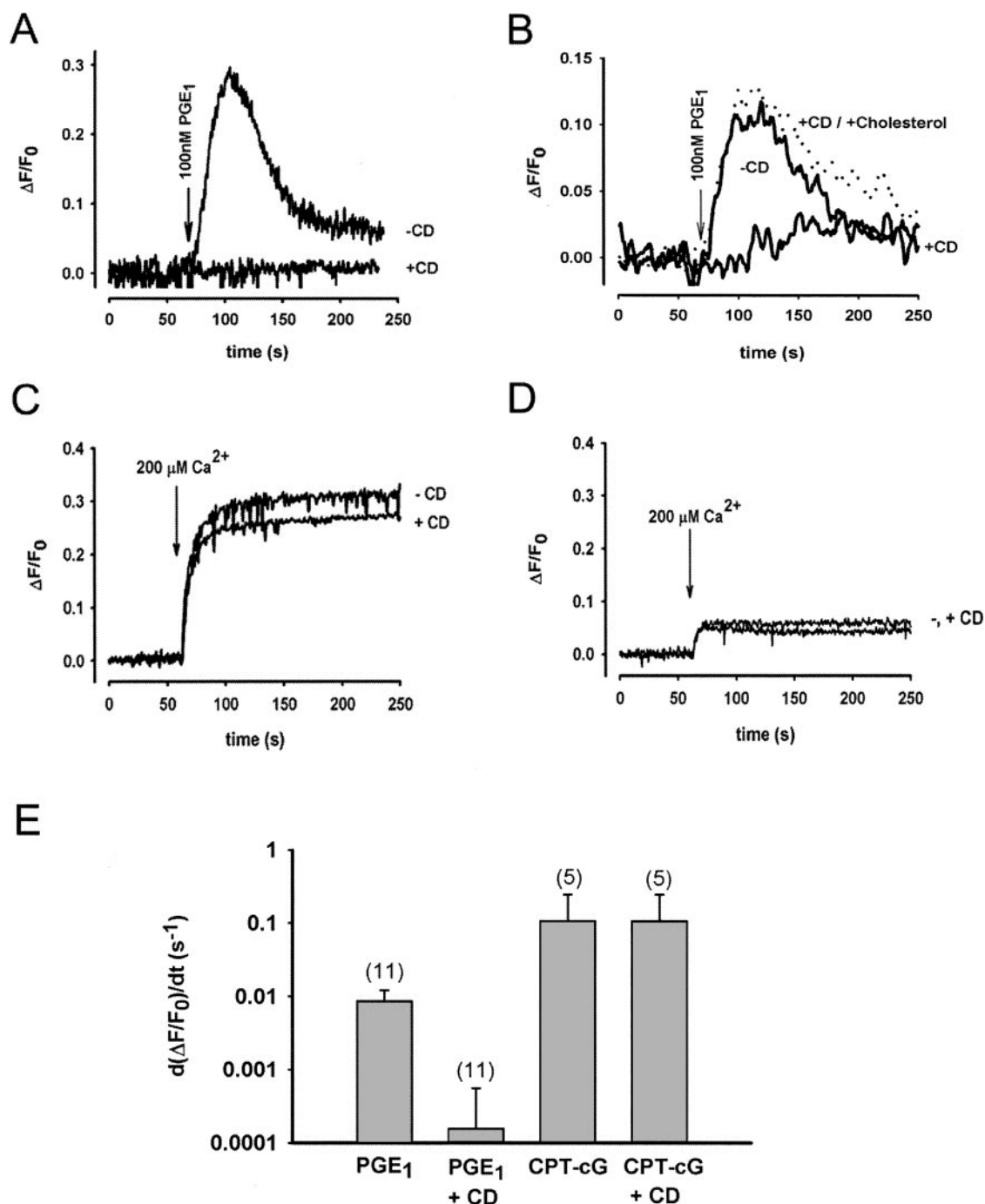
Fig. 5. Cholesterol depletion abolishes PGE_1-stimulated CNGA2 channel activity in intact cells. A–D, the fluorescent indicator fura-2 was used to monitor Ca^{2+} influx in HEK 293 cell populations expressing CNGA2. In this assay, an increase in local cAMP concentration causes activation of homomeric CNGA2 channels and a subsequent increase in Ca^{2+} entry. Ca^{2+} influx causes a decrease in fluorescence (ΔF), which was expressed relative to the prestimulus fluorescence (F_0). $\Delta F/F_0$ was plotted with inverted polarity so that increases in Ca^{2+} influx are represented as positive deflections. A, 100 nM PGE_1 stimulated an increase in calcium influx through CNGA2 channels ($-CD$, $n = 11$). Pretreatment of cells with 2% CD eliminated the response ($+CD$, $n = 11$). B, pretreatment of cells with 2% CD and 1 mM cholesterol ($+CD/+Cholesterol$) blocked the effect of 2% CD pretreatment alone ($+CD$). C, incubation in supersaturating (1 mM) CPT-cGMP for 1 h followed by the addition of 200 μM Ca^{2+} stimulated an increase in calcium influx ($-CD$, $n = 5$) that was only mildly reduced by pretreatment of cells with 2% CD ($+CD$, $n = 5$). D, only a small calcium influx was observed in uninfected cells after incubation in CPT-cGMP (1 mM) and addition of 200 μM Ca^{2+}, both with and without 2% CD pretreatment. E, bar graph showing the maximal rate of calcium influx for the experiments shown in A and C. Bars represent the averages from the number of experiments shown above the bar, and error bars represent the standard deviations. CD pretreatment significantly reduced the calcium influx after PGE_1 stimulation (t test, $p < 0.00001$).

greater shift in apparent affinity. Together, our results indicate that the local lipid environment of the CNGA2 channel profoundly affects its participation in cyclic nucleotide signaling by regulating channel function.

Although the effect of cholesterol depletion on the apparent affinity of CNGA2 channels for cAMP was variable, in most patches the effect was quite remarkable, with a >10-fold shift in affinity in some recordings. Further experiments are

required to establish whether cholesterol depletion affects the intrinsic affinity for cAMP or the allosteric conformational changes involved in channel opening. Cholesterol depletion almost certainly disrupts interactions between the channel and the lipid bilayer, either in the form of specific protein-lipid interactions or through changes in the physical properties of the bilayer itself (Martinac and Hamill, 2002). For example, a recent report suggests that interactions between membrane lipids and the hydrophobic transmembrane helices of ion channels directly influence channel properties (Valiyaveetil et al., 2002). There is also precedence for a role of lipid signaling molecules such as DAG and all-*trans* retinal in the modulation of CNG channel function (Crary et al., 2000; Dean et al., 2002).

It is also likely that the functional significance of lipid raft localization includes the compartmentation of ion channels with regulatory proteins (Simons and Toomre, 2000). Serine phosphorylation of the CNGA2 subunit near the calmodulin binding site on the carboxy terminus increases the sensitivity of CNGA2 channels to cyclic nucleotides (Muller et al., 1998). Lipid raft perturbation may destroy an association between CNGA2 channels and raft-associated kinases or other proteins to lower the apparent cAMP affinity (Brown et al., 2000; Kramer and Molokanova, 2001).

It is clear that the spatial and temporal confinement of signaling proteins is a general mechanism for coordinating cellular function by preventing cross talk between competing pathways. Compartmentalized cyclic nucleotide signaling in three dimensions is necessary to explain differential regulation of cellular targets by cAMP and to ensure rapid and efficient activation of CNG channels (Rich et al., 2000, 2001a). It is tempting to hypothesize a role for lipid rafts in the establishment and/or maintenance of these restricted microdomains. Certainly, there is increasing evidence that rafts organize cAMP signaling proteins. For instance, many of the components involved in cAMP-mediated signaling, in-
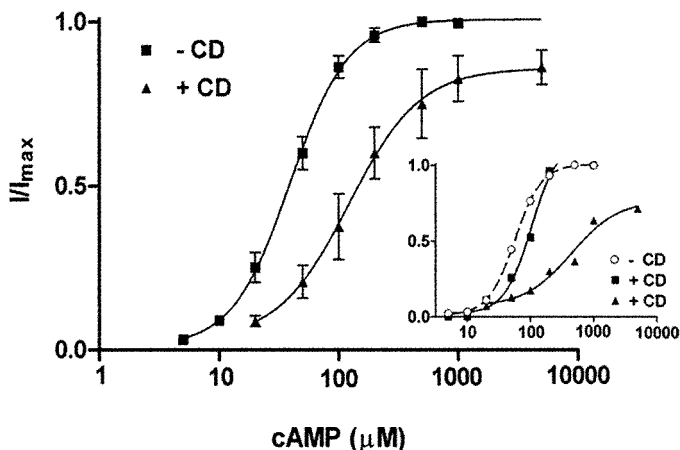
cluding G-protein-coupled receptors, certain G-protein isoforms, and some adenylyl cyclases, associate with lipid rafts in a diverse number of cell types (Schwencke et al., 1999; Moffett et al., 2000; Rybin et al., 2000; Cordeaux and Hill, 2002; Lamb et al., 2002; Ostrom et al., 2002). In addition, some reports suggest that lipid raft perturbation disrupts G-protein mediated cAMP accumulation (Fagan et al., 2000; Rybin et al., 2000; Smith et al., 2002). Therefore, association of CNGA2 with lipid rafts may be a mechanism for ensuring proximity to effector molecules within restricted plasma membrane microdomains. Our finding that CNGA2 channel activation after PGE_1-stimulation is disrupted by cholesterol depletion suggests that prostaglandin receptors and CNGA2 channels exist together within a cholesterol-rich membrane microdomain. If so, we predict that specific prostaglandin receptor subtypes also associate with biochemically-isolated lipid rafts and that they reside in close proximity to CNGA2 channels at the plasma membrane. Further work is necessary to test these predictions.

Although our data strongly support the idea that the integrity of cholesterol-rich raft membranes is important for CNGA2 channel function, it is possible that not all CNGA2 channels are localized to lipid raft microdomains. Although the amount of CNGA2 in soluble gradient fractions correlates well with the level of intracellular protein in transfected HEK 293 cells, it may also reflect the existence of channel protein in nonraft domains at the plasma membrane. Again, it is important to note that the biochemical isolation of lipid rafts is a qualitative, not a quantitative, assessment of protein affinity for cholesterol-rich, detergent-insoluble membranes (Shogomori and Brown, 2003). For this reason, it is difficult to calculate the fraction of CNGA2 that resides in raft and nonraft membranes based on our biochemical data. However, the variability in the effect of methyl-β-cyclodextrin on the apparent affinity of CNGA2 channels supports the idea that channels exist in both raft and nonraft environments, and it is the PGE_1-stimulated channel that is compartmentalized in rafts and sensitive to cholesterol depletion. It will be interesting to determine whether agonists for other G-protein-coupled receptors activate CNGA2 channels that are insensitive to cholesterol depletion.

The localization of CNG channels to lipid rafts may play a role in organizing cyclic nucleotide-mediated signaling compartments in neurons of the olfactory epithelium. Schreiber et al. (2000) demonstrated that the G-protein and adenylyl cyclase isoforms involved in odorant signaling associate with lipid rafts. The affinity of odorant signaling proteins and CNG channels for physically distinct lipid raft membranes may facilitate their coassembly into signaling microdomains. Additionally, lipid rafts may play a role in targeting the channel and signaling proteins to defined regions of the dendritic cilia. Schreiber et al. (2000) also reported that the olfactory G protein and adenylyl cyclase type III bind caveolin and that disruption of caveolin binding inhibits odorant-induced cAMP production in OSNs. Although we found no direct interaction between CNGA2 and caveolin in rat olfactory membranes, we cannot exclude the possibility that the native olfactory CNG channel localizes to caveolae in vivo. Further work with CNG channels in OSNs is required to clarify the involvement of caveolin.

The large shift in the apparent affinity of CNGA2 channels for cAMP after cholesterol depletion may have physiological

Fig. 6. Cholesterol depletion reduces the apparent cAMP binding affinity of CNGA2 channels in isolated patches. CNGA2 channel activity was measured in inside-out patches pulled from HEK 293 cells expressing wtCNGA2 either before or after treatment with 2% CD for 15 to 30 min at 37°C. Currents activated by bath application of increasing concentrations of cAMP (5–5000 μM) were measured at +50 mV, and the current at each cAMP concentration was expressed relative to the maximal current activated by 1 mM cGMP. The inset shows representative examples of single patch recordings from untreated cells (○) and those treated with 2% CD (closed symbols). All curves are fit to the Hill equation. The average $K_{1/2}$ increased from approximately 39 to 123 μM after CD incubation. Error bars represent S.E.M.

significance for olfactory signaling. Modulation of channel cAMP affinity is believed to provide the main adaptive feedback mechanism for desensitization of the olfactory signaling pathway (Balasubramanian et al., 1996; Kurahashi and Menini, 1997). Our results suggest that alteration of membrane lipid, either by disease or by clinical use of lipid-lowering drugs, can affect olfaction by altering the function of raft-localized CNG channels.

References

Anderson RG (1998) The caveolae membrane system. *Annu Rev Biochem* **67**:199–225.

Balasubramanian S, Lynch JW, and Barry PH (1996) Calcium-dependent modulation of the agonist affinity of the mammalian olfactory cyclic nucleotide-gated channel by calmodulin and a novel endogenous factor. *J Membr Biol* **152**:13–23.

Baylor DA, Lamb TD, and Yau KW (1979) The membrane current of single rod outer segments. *J Physiol* **288**:589–611.

Benting JH, Rietveld AG, and Simons K (1999) N-glycans mediate the apical sorting of a GPI-anchored, raft-associated protein in Madin-Darby canine kidney cells. *J Cell Biol* **146**:313–320.

Bonigk W, Bradley J, Muller F, Sesti F, Boekhoff I, Ronnett GV, Kaupp UB, and Frings S (1999) The native rat olfactory cyclic nucleotide-gated channel is composed of three distinct subunits. *J Neurosci* **19**:5332–5347.

Bradley J, Li J, Davidson N, Lester HA, and Zinn K (1994) Heteromeric olfactory cyclic nucleotide-gated channels: a subunit that confers increased sensitivity to cAMP. *Proc Natl Acad Sci USA* **91**:8890–8894.

Bravo-Zehnder M, Orio P, Norambuena A, Wallner M, Meera P, Toro L, Latorre R, and Gonzalez A (2000) Apical sorting of a voltage- and Ca²⁺-activated K⁺ channel alpha-subunit in Madin-Darby canine kidney cells is independent of N-glycosylation. *Proc Natl Acad Sci USA* **97**:13114–13119.

Brown DA and London E (1998) Structure and origin of ordered lipid domains in biological membranes. *J Membr Biol* **164**:103–114.

Brown RL, Haley TL, and Snow SD (2000) Irreversible activation of cyclic nucleotide-gated ion channels by sulfhydryl-reactive derivatives of cyclic GMP. *Biochemistry* **39**:432–441.

Cordeaux Y and Hill SJ (2002) Mechanisms of cross-talk between G-protein-coupled receptors. *Neurosignals* **11**:45–57.

Crary JI, Dean DM, Nguitragool W, Kurshan PT, and Zimmerman AL (2000) Mechanism of inhibition of cyclic nucleotide-gated ion channels by diacylglycerol. *J Gen Physiol* **116**:755–768.

Dean DM, Nguitragool W, Miri A, McCabe SL, and Zimmerman AL (2002) All-trans-retinal shuts down rod cyclic nucleotide-gated ion channels: a novel role for photoreceptor retinoids in the response to bright light? *Proc Natl Acad Sci USA* **99**:8372–8377.

Fagan KA, Smith KE, and Cooper DM (2000) Regulation of the Ca²⁺-inhibitable adenylyl cyclase type VI by capacitative Ca²⁺ entry requires localization in cholesterol-rich domains. *J Biol Chem* **275**:26530–26537.

Fesenko EE, Kolesnikov SS, and Lyubarsky AL (1985) Induction by cyclic GMP of cationic conductance in plasma membrane of retinal rod outer segment. *Nature (Lond)* **313**:310–313.

Finn JT, Grunwald ME, and Yau KW (1996) Cyclic nucleotide-gated ion channels: an extended family with diverse functions. *Annu Rev Physiol* **58**:395–426.

Firestein S and Werblin F (1989) Odor-induced membrane currents in vertebrate-olfactory receptor neurons. *Science (Wash DC)* **244**:79–82.

Foster LJ, De Hoog CL, and Mann M (2003) Unbiased quantitative proteomics of lipid rafts reveals high specificity for signaling factors. *Proc Natl Acad Sci USA* **100**:5813–5818.

Furuchi T and Anderson RG (1998) Cholesterol depletion of caveolae causes hyperactivation of extracellular signal-related kinase (ERK). *J Biol Chem* **273**:21099–21104.

Griffith LC (2001) Potassium channels: the importance of transport signals. *Curr Biol* **11**:R226–R228.

Harder T, Scheiffele P, Verkade P, and Simons K (1998) Lipid domain structure of the plasma membrane revealed by patching of membrane components. *J Cell Biol* **141**:929–942.

Kaupp UB and Seifert R (2002) Cyclic nucleotide-gated ion channels. *Physiol Rev* **82**:769–824.

Kramer RH and Molokanova E (2001) Modulation of cyclic-nucleotide-gated channels and regulation of vertebrate phototransduction. *J Exp Biol* **204**:2921–2931.

Kurahashi T and Menini A (1997) Mechanism of odorant adaptation in the olfactory receptor cell. *Nature (Lond)* **385**:725–729.

Lamb ME, Zhang C, Shea T, Kyle DJ, and Leeb-Lundberg LM (2002) Human B1 and B2 bradykinin receptors and their agonists target caveolae-related lipid rafts to different degrees in HEK293 cells. *Biochemistry* **41**:14340–14347.

Liman ER and Buck LB (1994) A second subunit of the olfactory cyclic nucleotide-gated channel confers high sensitivity to cAMP. *Neuron* **13**:611–621.

Magee T, Pirinen N, Adler J, Pagakis SN, and Parmryd I (2002) Lipid rafts: cell surface platforms for T cell signaling. *Biol Res* **35**:127–131.

Martens JR, Navarro-Polanco R, Coppock EA, Nishiyama A, Parshley L, Grobaski TD, and Tamkun MM (2000) Differential targeting of Shaker-like potassium channels to lipid rafts. *J Biol Chem* **275**:7443–7446.

Martinac B and Hamill OP (2002) Gramicidin A channels switch between stretch activation and stretch inactivation depending on bilayer thickness. *Proc Natl Acad Sci USA* **99**:4308–4312.

Moffett S, Brown DA, and Linder ME (2000) Lipid-dependent targeting of G proteins into rafts. *J Biol Chem* **275**:2191–2198.

Muller F, Bonigk W, Sesti F, and Frings S (1998) Phosphorylation of mammalian olfactory cyclic nucleotide-gated channels increases ligand sensitivity. *J Neurosci* **18**:164–173.

Nakamura T and Gold GH (1987) A cyclic nucleotide-gated conductance in olfactory receptor cilia. *Nature (Lond)* **325**:442–444.

Ostermeyer AG, Beckrich BT, Ivarson KA, Grove KE, and Brown DA (1999) Glycosphingolipids are not essential for formation of detergent-resistant membrane rafts in melanoma cells. Methyl-β-cyclodextrin does not affect cell surface transport of a GPI-anchored protein. *J Biol Chem* **274**:34459–34466.

Ostrom RS, Liu X, Head BP, Gregorian C, Seasholtz TM, and Insel PA (2002) Localization of adenylyl cyclase isoforms and G protein-coupled receptors in vascular smooth muscle cells: expression in caveolin-rich and noncaveolin domains. *Mol Pharmacol* **62**:983–992.

Rich TC, Fagan KA, Nakata H, Schaack J, Cooper DM, and Karpen JW (2000) Cyclic nucleotide-gated channels colocalize with adenylyl cyclase in regions of restricted cAMP diffusion. *J Gen Physiol* **116**:147–161.

Rich TC, Fagan KA, Tse TE, Schaack J, Cooper DM, and Karpen JW (2001a) A uniform extracellular stimulus triggers distinct cAMP signals in different compartments of a single cell. *Proc Natl Acad Sci USA* **98**:13049–13054.

Rich TC, Tse TE, Rohan JG, Schaack J, and Karpen JW (2001b) In vivo assessment of local phosphodiesterase activity using tailored cyclic nucleotide-gated channels as cAMP sensors. *J Gen Physiol* **118**:63–78.

Rybin VO, Xu X, Lisanti MP, and Steinberg SF (2000) Differential targeting of β-adrenergic receptor subtypes and adenylyl cyclase to cardiomyocyte caveolae. A mechanism to functionally regulate the cAMP signaling pathway. *J Biol Chem* **275**:41447–41457.

Sautter A, Zong X, Hofmann F, and Biel M (1998) An isoform of the rod photoreceptor cyclic nucleotide-gated channel beta subunit expressed in olfactory neurons. *Proc Natl Acad Sci USA* **95**:4696–4701.

Savchenko A, Barnes S, and Kramer RH (1997) Cyclic-nucleotide-gated channels mediate synaptic feedback by nitric oxide. *Nature (Lond)* **390**:694–698.

Schreiber S, Fleischer J, Breer H, and Boekhoff I (2000) A possible role for caveolin as a signaling organizer in olfactory sensory membranes. *J Biol Chem* **275**:24115–24123.

Schwencke C, Yamamoto M, Okumura S, Toya Y, Kim SJ, and Ishikawa Y (1999) Compartmentation of cyclic adenosine 3′,5′-monophosphate signaling in caveolae. *Mol Endocrinol* **13**:1061–1070.

Seno K, Kishimoto M, Abe M, Higuchi Y, Mieda M, Owada Y, Yoshiyama W, Liu H, and Hayashi F (2001) Light- and guanosine 5′-3-O-(thio)triphosphate-sensitive localization of a G protein and its effector on detergent-resistant membrane rafts in rod photoreceptor outer segments. *J Biol Chem* **276**:20813–20816.

Shogomori H and Brown DA (2003) Use of detergents to study membrane rafts: the good, the bad and the ugly. *Biol Chem* **384**:1259–1263.

Simons K and Ikonen E (1997) Functional rafts in cell membranes. *Nature (Lond)* **387**:569–572.

Simons K and Toomre D (2000) Lipid rafts and signal transduction. *Nat Rev Mol Cell Biol* **1**:31–39.

Smart EJ, Ying YS, Mineo C, and Anderson RG (1995) A detergent-free method for purifying caveolae membrane from tissue culture cells. *Proc Natl Acad Sci USA* **92**:10104–10108.

Smith KE, Gu C, Fagan KA, Hu B, and Cooper DM (2002) Residence of adenylyl cyclase type 8 in caveolae is necessary but not sufficient for regulation by capacitative Ca²⁺ entry. *J Biol Chem* **277**:6025–6031.

Sowa G, Pypaert M, and Sessa WC (2001) Distinction between signaling mechanisms in lipid rafts vs. caveolae. *Proc Natl Acad Sci USA* **98**:14072–14077.

Trudeau MC and Zagotta WN (2002) An intersubunit interaction regulates trafficking of rod cyclic nucleotide-gated channels and is disrupted in an inherited form of blindness. *Neuron* **34**:197–207.

Valiyaveetil FI, Zhou Y, and MacKinnon R (2002) Lipids in the structure, folding and function of the KcsA K⁺ channel. *Biochemistry* **41**:10771–10777.

Weitz D, Ficek N, Kremmer E, Bauer PJ, and Kaupp UB (2002) Subunit stoichiometry of the CNG channel of rod photoreceptors. *Neuron* **36**:881–889.

Zheng J, Trudeau MC, and Zagotta WN (2002) Rod cyclic nucleotide-gated channels have a stoichiometry of three CNGA1 subunits and one CNGB1 subunit. *Neuron* **36**:891–896.

Zhong H, Molday LL, Molday RS, and Yau KW (2002) The heteromeric cyclic nucleotide-gated channel adopts a 3A:1B stoichiometry. *Nature (Lond)* **420**:193–198.

Address correspondence to: Jeffrey R. Martens, Dept. of Physiology and Pharmacology, Oregon Health & Science University, 3181 SW Sam Jackson Park Road, L334, Portland, OR 97239-3098. E-mail: martensj@ohsu.edu